**The Effect of sand/cement ratio and silica fume on the microstructure of mortars**

Feldman, R. F.



**Publisher's version / Version de l'éditeur:**
https://doi.org/10.1016/0008-8846(86)90065-7
*Cement and Concrete Research, 16, January 1, pp. 31-39, 1986-01-01*

National Research Council Canada
Conseil national de recherches Canada

Institute for Research in Construction
Institut de recherche en construction

# The Effect of Sand/Cement Ratio and Silica Fume on the Microstructure of Mortars

by R.F. Feldman



Reprinted from
Cement and Concrete Research
Vol. 16, No. 1, 1986
p. 31 - 39
(IRC Paper No. 1358)

Price $2.75

NRCC 25543



Canada

RÉSUMÉ

On a préparé des mortiers contenant 0 et 10 p. cent de silice fine avec des rapports eau/ciment + silice de 0.60 et sable/ciment de 0, 0.5, 1.0, 1.5, 1.8, 2.0, 2.25 et 3.0. La répartition des pores a été étudiée par injection de mercure et par réinjection. Il se forme davantage de pores de (97→0.175) × $10^3$ nm à l'interface du sable pour les mortiers contenant de la silice fine que pour les autres. Il n'existe qu'une très faible différence dans la répartition des pores avec ou sans silice fine.

CEMENT and CONCRETE RESEARCH. Vol. 16, pp. 31-39, 1986. Printed in the USA.
0008-8846/86 $3.00+00. 

# THE EFFECT OF SAND/CEMENT RATIO AND SILICA FUME ON THE MICROSTRUCTURE OF MORTARS

R.F. Feldman
Division of Building Research
National Research Council of Canada
Ottawa, Ontario, K1A 0R6

(Communicated by J.P. Skalny)
(Received July 16, 1985)

ABSTRACT

Cement mortars containing 0 and 10% silica fume were prepared at a water/cement + silica fume ratio of 0.60 and sand/cement ratios of 0, 0.5, 1.0, 1.5, 1.8, 2.0, 2.25 and 3.0. Pore-size distributions were studied by mercury intrusion and reintrusion. More pores of $(97 \rightarrow 0.175) \times 10^3$ nm size form at the sand interface for mortars with silica fume than without it. There is only a slight difference in the fine pore distribution with and without silica fume.

## Introduction

Studies of portland cement paste and equivalent mortars show that the sand-matrix interface has a definite effect on the pore-size distribution (1-3). Further work with portland cement - silica fume blends has demonstrated that the effect at the interface is magnified in this system (1). Addition of silica fume in pastes affects the hydration rate (4). The freeze-thaw resistance is not affected, although it is greatly improved in mortars with sand/cement ratio of 2.25 (3). Pore volume with diameters in the $(97 \rightarrow 0.875) \times 10^3$ nm range is greatly increased by the addition of silica fume to mortar with sand/cement ratio of 2.25. These pores may occur at the sand-matrix interface due to the interaction of silica fume and $Ca(OH)_2$, which initially forms at the interface; a portion of these pores may not be as readily accessible to fluids (1,3).

Well-cured blends of several waste materials and portland cement have lower permeabilities than pastes or concretes without the addition, and have demonstrated superior resistance to various forms of chemical attack (5-8). Silica fume, in addition to causing very low permeabilities in blends, is a very reactive pozzolan (4,8). The sequence of reactions leading to a unique pore-size distribution in mortars can provide a material capable of resisting many forms of chemical and physical attack and of protecting other susceptible materials such as reinforcing steel.

In this work, a detailed study was made of the pore structure of mortars with sand/cement ratios varying from 0 to 3.0, with and without the replacement of 10% portland cement by silica fume.

## Experimental

### Materials

Type I portland cement with $C_3A$ content of 11.82% and silica fume containing 95.2% $SiO_2$, 1.56% carbon, 0.27% $K_2O$ and 0.10% $Na_2O$ (surface area 21 000 $m^2/kg$) were used. Ottawa silica sand passing ASTM C 109 was used for mortar with sand/binder ratios of 0, 0.5, 1.0, 1.5, 1.8, 2.0, 2.25 and 3.0. Binder in the mortar contained 0 or 10% silica fume. Mixes were prepared at w/(c+sf) of 0.60 (w = water, c = cement, sf = silica fume). No water-reducing or air-entraining admixtures were used.

### Mixing

Cement, silica fume and water were mixed for 30 seconds in the bowl of a Hobart Model N-50 mixer (ASTM C 305) at a slow speed. All the sand was added and mixing continued at slow speed for 30 seconds. The mixer was stopped and then mixing was continued at medium speed for 30 seconds, after which the mix was allowed to stand for 1½ minutes. Mixing was then completed by a further one minute at medium speed.

### Properties determined

Pore-size distribution was determined in all mixes after 28 days of curing time (Hg porosimetry to a pressure of 414 MPa). Specimens were dried by vacuum and final heating for about 24 h at 100°C. Mercury was removed by heating specimens at 105°C in vacuum for several weeks until weight returned to original value. Reintrusion was performed on mixes containing silica fume at sand/cement ratios of 0, 1.5, 1.8, 2.0, 2.25 and 3.0.

## Results

### Pore-size distribution of mortars without silica fume

Results for the pore-size distribution of mortars with sand/cement ratios of 0, 1.5, 1.8, 2.0, 2.25 and 3.0, cured for 28 days, without silica fume addition, prepared at a water/cement ratio of 0.6, are shown in Figure 1. Results of porosity are based on total volume of mortar sample. Total pore volumes down to 30 nm pore diameter for all the mortar mixes are larger than for paste (sand/cement ratio of 0.0). The mortar with sand/cement ratio of 3.0 has the maximum total porosity down to 500 nm pore diameter, but the paste has, by far, the maximum total porosity when all pores are included (down to 2.9 nm).

Pore volumes calculated in this way are not entirely meaningful, however, because, as sand content increases, an increasing proportion of the volume of the sample is non-porous sand and a decreasing proportion is cement paste, which contains the pores. In order to normalize these results, pore volume was calculated as a percent of the paste volume of the mortar. The sand volume was subtracted from the total volume of the original mixture; this was done by calculating volumes of components, using densities for the sand, cement and water. Results are presented in Figure 2. The total porosity at 2.9 nm now increases approximately with sand/cement ratio; the highest and lowest porosity is 40.0 and 35.6% for the 3.0 and 0.0 sand/cement ratio, respectively. However, the distribution of pores is vastly different; for the 0.0 sand/cement ratio, the pore volume down to 40 nm is only about 2.5%, while this value increases to 12, 19.5, 18.9, 20.5 and 21.2% for the sand/cement ratios of 1.5, 1.8, 2.0, 2.25 and 3.0, respectively.

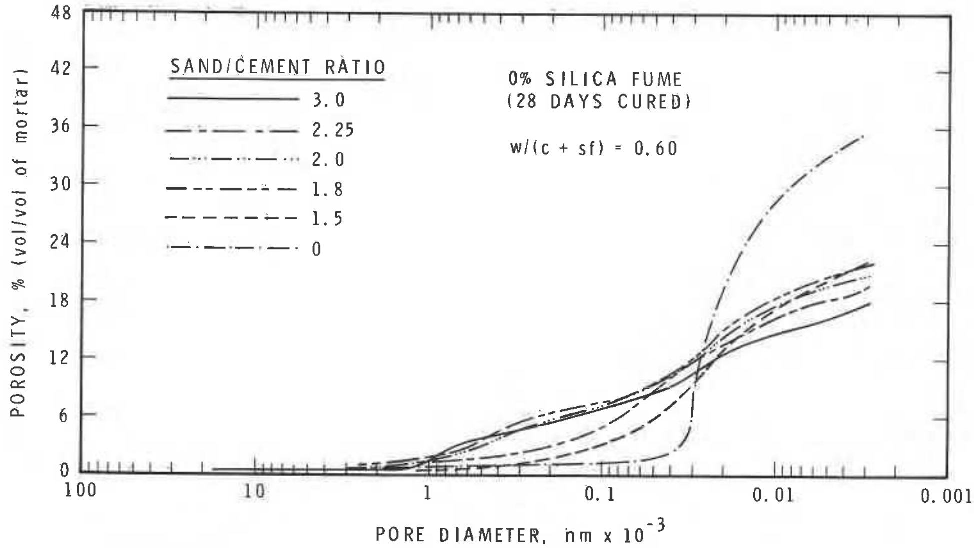


FIG. 1
Pore-size distribution of mortars plotted as volume percent of mortar. Sand/cement ratios = 0.0 to 3.0.

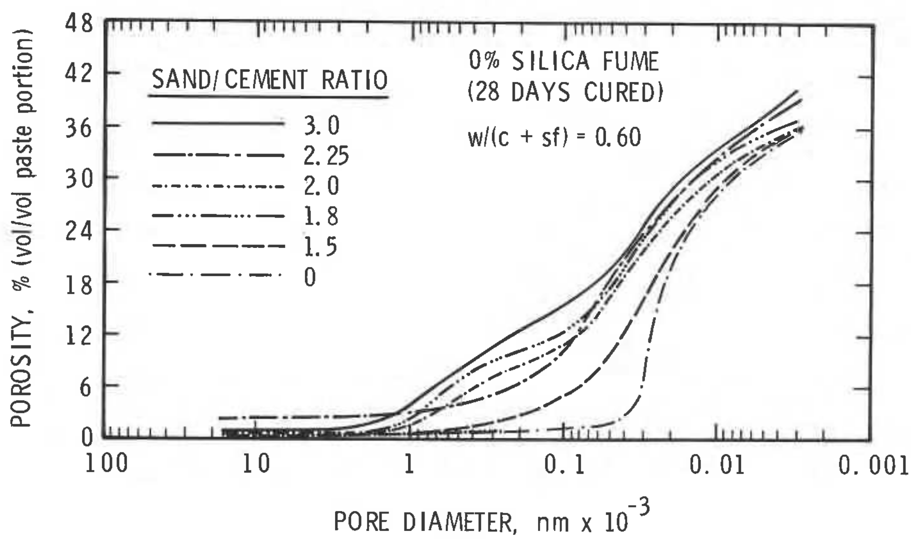


FIG. 2
Pore-size distribution of mortars plotted as volume percent of paste portion. Sand/cement ratios = 0.0 to 3.0.

The pore volume is divided into four ranges of pore diameters: (97→0.875, 0.875→0.175, 0.175→0.0175, 0.0175→0.0029) ~ $10^3$ nm. These are presented in Table I, calculated both on the basis of total mortar volume and paste volume alone. With some deviation in the 1.8 to 2.25 sand/cement ratio ranges, the two coarser pore ranges increase in volume with sand/cement ratio, and the two finer ranges decrease. The volume of each of the coarse ranges and the sum of volumes of these ranges is plotted against sand/cement ratio in Figure 3.

TABLE I
Pore-size Distribution of Mortars. Sand/cement Ratio = 0.0 to 3.0.
0% Silica Fume. w/(c+sf) = 0.60. 28 Days Cured.

| Sand/cement ratio | 3.0 | | 2.25 | | 2.0 | |
|---|---|---|---|---|---|---|
| Pore diameter ($nm \times 10^{-3}$) | Normal | Paste portion | Normal | Paste portion | Normal | Paste portion |
| 97→0.875 | 1.79 | 4.04 | 1.22 | 2.37 | 1.14 | 2.10 |
| 0.875→0.175 | 3.89 | 8.79 | 2.3 | 4.47 | 3.40 | 6.25 |
| 0.175→0.0175 | 7.15 | 16.15 | 10.85 | 21.08 | 9.45 | 17.37 |
| 0.0175→0.0029 | 4.60 | 11.00 | 5.81 | 11.29 | 5.26 | 9.67 |
| TOTAL | 17.43 | 39.98 | 20.18 | 39.21 | 19.25 | 35.39 |
| | 1.8 | | 1.5 | | 0.0 | |
| | Normal | Paste portion | Normal | Paste portion | Normal | |
| 97→0.875 | 1.64 | 2.88 | 0.18 | 0.29 | 0.57 | |
| 0.875→0.175 | 4.37 | 7.67 | 1.71 | 2.79 | 0.55 | |
| 0.175→0.0175 | 9.65 | 16.83 | 11.66 | 19.0 | 19.84 | |
| 0.0175→0.0029 | 5.38 | 9.44 | 8.2 | 13.36 | 14.88 | |
| TOTAL | 21.04 | 36.92 | 21.75 | 35.43 | 35.84 | |

Pore-size distribution of mortars with silica fume on first intrusion

The pore-diameter distribution of mortars containing 10% silica fume (cured for 28 days), with sand/cement ratios of 0.0, 0.5, 1.0, 1.5, 1.8, 2.0, 2.25 and 3.0, is presented in Figure 4. Volume calculations are based on paste portion. Whereas features imposed on the curves due to the influence of silica fume are evident (1), there is considerable difference between the mortars, although the total pore volume only varies between approximately 39.0 and 44.0% by volume. The influence of silica fume may be observed in Table II, where the pore volumes for the four pore ranges are calculated, on the basis of both the total mortar volume and the volume of the paste portion. Generally, the volume of pore diameter ranges (97→0.875 and 0.875→0.175) $\times 10^3$ nm (the coarser ranges) and (0.0175→0.0029) $\times 10^3$ nm (the finest range) increases and that of the (0.175→0.0175) $\times 10^3$ nm range decreases as silica fume is added.

The volume of the pores in the two coarser ranges and the sum of these volumes are plotted against sand/cement ratio in Figure 3B. In the

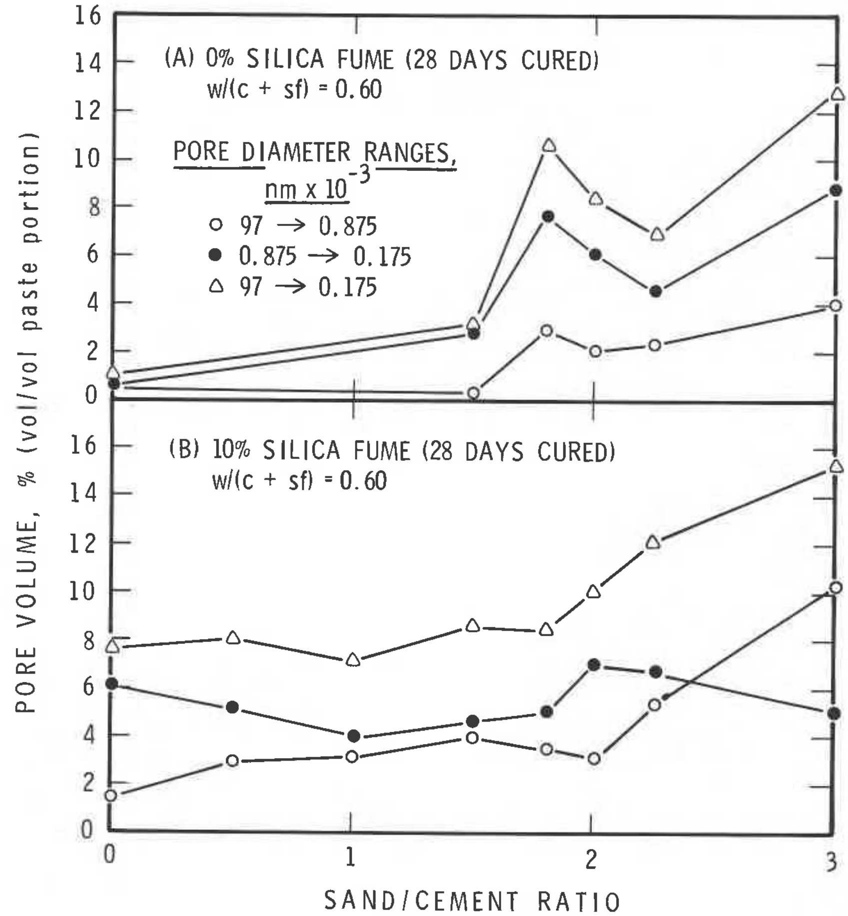


FIG. 3
Plot of pore volumes (% of paste portion) of various pore size ranges of mortars vs sand/cement ratios (0.0 to 3.0).

(97→0.875) × $10^3$ nm range, the volume increases generally with sand/cement ratio, with a steep increase after a sand/cement ratio of 2.0. These values are also greater in each case than the volumes for the specimens without silica fume addition. The volumes for the range (0.875→0.175) × $10^3$ nm vary in a somewhat random manner with sand/cement ratio within 4 to 7% pore volume. These values up to 1.5 sand/cement ratio are in excess of those for specimens without silica fume, but values for 1.8 and 3.0 sand/cement ratio are lower.

The sum of the two ranges (97→0.875) and (0.875→0.175) × $10^3$ nm are also shown in Figure 3B. Only a small change in volume of pores occurs from 0 to 1.8 sand/cement ratio but beyond 1.8 the increase is quite abrupt; values increase from an average of about 8% for sand/cement ratio up to 1.8, to over 15% for the specimen with a ratio of 3.0.

Pore-size distribution of mortars with silica fume on reintrusion

The pore diameter distributions on reintrusion for the mortars containing 10% silica fume with sand/cement ratios of 0.0, 1.5, 1.8, 2.0, 2.25

TABLE II
Pore-size Distribution of Mortars. Sand/cement Ratio = 0.0 to 3.0.
10% Silica Fume. w/(c+sf) = 0.60. 28 Days Cured.

| Sand/cement ratio | 3.0 | | 2.25 | | 2.0 | | 1.8 | |
|---|---|---|---|---|---|---|---|---|
| Pore diameter (nm × $10^{-3}$) | Normal | Paste portion | Normal | Paste portion | Normal | Paste portion | Normal | Paste portion |
| 97→0.875 | 4.6 | 10.30 | 2.78 | 5.36 | 1.69 | 3.09 | 1.98 | 3.45 |
| 0.875→0.175 | 2.21 | 4.95 | 3.47 | 6.69 | 3.83 | 6.99 | 2.87 | 5.00 |
| 0.175→0.0175 | 4.40 | 9.86 | 9.04 | 17.44 | 7.96 | 14.54 | 8.17 | 14.25 |
| 0.0175→0.0029 | 8.41 | 18.83 | 7.99 | 15.42 | 9.2 | 16.80 | 9.47 | 16.51 |
| TOTAL | 19.62 | 43.93 | 23.28 | 44.92 | 22.68 | 41.42 | 22.49 | 39.21 |

| | 1.5 | | 1.0 | | 0.5 | | 0.0 |
|---|---|---|---|---|---|---|---|
| | Normal | Paste portion | Normal | Paste portion | Normal | Paste portion | Normal |
| 97→0.875 | 2.49 | 4.03 | 2.24 | 3.17 | 2.44 | 2.94 | 1.52 |
| 0.875→0.175 | 2.83 | 4.58 | 2.81 | 3.97 | 4.22 | 5.09 | 6.13 |
| 0.175→0.0175 | 8.7 | 14.09 | 9.2 | 13.0 | 9.9 | 11.95 | 10.89 |
| 0.0175→0.0029 | 9.93 | 16.08 | 13.34 | 18.85 | 15.83 | 19.09 | 20.64 |
| TOTAL | 23.95 | 38.79 | 27.59 | 38.99 | 32.39 | 39.08 | 39.18 |

and 3.0 are presented in Table III. In each case there is a large increase in the volume of pores in the coarse range [(97→0.875) × $10^3$ nm] compared to first intrusion (Table II), the increase being greater with larger sand/cement ratios. The volume contained in the two smallest pore ranges is generally lower for the reintrusion distribution than for the first distribution.

A comparison of pore distributions between the reintruded specimen containing silica fume (Table III) and the equivalent specimen without silica fume (first intrusion, Table I) reveals that, with the exception of the range (97→0.875) × $10^3$ nm, they are similar. The specimens prepared at a sand/cement ratio of 2.0 are typical of the specimens measured. In the (0.0175→0.0029) × $10^3$ nm range the volume for the reintruded specimen with silica fume is 12.13% compared to 9.67% for the specimen without silica fume; in the range (0.175→0.0175) × $10^3$ nm, the corresponding values are 14.02% to 17.37%; in the range (0.875→0.175) × $10^3$ nm, 6.30 to 6.25%; and in the range (97→0.875) × $10^3$ nm, 10.74 to 2.10%. The total porosities are 43.19 to 35.39%.

## Discussion

The marked difference in the pore distribution of mortars as a function of sand/cement ratio appears to be an interfacial effect. As the sand/cement ratio increases, the amount of interface per volume of specimen should increase and larger pores may be formed around the sand grain during mixing.

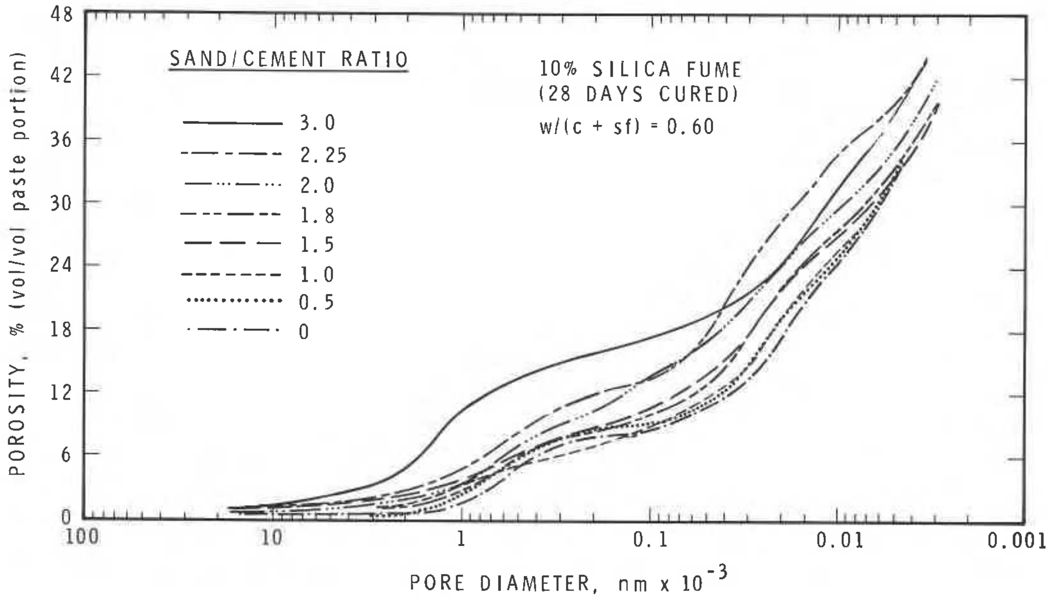


FIG. 4
Pore-size distribution of mortars plotted as volume percent of paste portion. Sand/cement ratios = 0.0 to 3.0.

However, other factors may contribute to this phenomenon. It has been shown that during hydration a preferential deposition of $Ca(OH)_2$ occurs in the interfacial zone (less than 50 microns) around aggregates in concrete and around fibres or sand in mortars (9-11). The layer of $Ca(OH)_2$ may be covered with a layer of elongated C-S-H gel particles. These layers have been referred to as a duplex film (9) and the zone nearest the film is only sparsely occupied at early stages of hydration. Larger $Ca(OH)_2$ crystals may develop in this zone after a few days of hydration. This modified form of deposition of products is likely to cause changes to the pore distribution.

Effects of inclusions on hydration rates and degree of hydration have been reported (4,12); inclusions may also have an effect on pore distribution. $Ca(OH)_2$ reduction in the matrix due to its deposition at interfaces can reduce permeability of the body and access to cement grains by $H_2O$; this may result in limited hydration relative to mixes without sand and can account for increased porosity (4).

The addition of silica fume will further influence the process of product crystallization around interfaces (1,4); the silica reacts with the $Ca(OH)_2$ starting at early times of hydration, creating both a better bond with the aggregate-matrix interface and larger pores in the vicinity of the matrix. Some of the $Ca(OH)_2$ crystallized around sand grains may redissolve to react with the relatively insoluble silica in locations away from the interface.

The removal of $Ca(OH)_2$ from the matrix and interface decreases the permeability of the specimen (2,5,6) and the degree of hydration of the cement, resulting in a higher porosity (4,12). The low permeability can be achieved despite a higher porosity by leaving a high degree of discontinuity

TABLE III
Pore-size Distribution of Mortars on Reintrusion.
Sand/cement Ratio = 0.0 to 3.0.
10% Silica Fume. w/(c+sf) = 0.60. 28 Days Cured.

| Sand/cement ratio | 3.0 | | 2.25 | | 2.0 | |
|---|---|---|---|---|---|---|
| Pore diameter ($nm \times 10^{-3}$) | Normal | Paste portion | Normal | Paste portion | Normal | Paste portion |
| 97→0.875 | 5.79 | 12.96 | 3.61 | 12.50 | 5.88 | 10.74 |
| 0.875→0.175 | 1.93 | 4.33 | 2.76 | 1.66 | 3.45 | 6.30 |
| 0.175→0.0175 | 4.51 | 10.09 | 8.28 | 12.50 | 7.68 | 14.02 |
| 0.0175→0.0029 | 5.79 | 12.97 | 8.70 | 12.90 | 6.64 | 12.13 |
| TOTAL | 18.02 | 40.35 | 23.35 | 39.56 | 23.65 | 43.19 |

| | 1.8 | | 1.5 | | 0.0 |
|---|---|---|---|---|---|
| | Normal | Paste portion | Normal | Paste portion | Normal |
| 97→0.875 | 4.86 | 8.47 | 74.87 | 7.89 | 2.80 |
| 0.875→0.175 | 3.25 | 5.67 | 3.08 | 4.98 | 7.14 |
| 0.175→0.0175 | 8.76 | 15.27 | 8.46 | 13.70 | 11.48 |
| 0.0175→0.0029 | 6.58 | 11.47 | 7.95 | 12.88 | 17.59 |
| TOTAL | 23.45 | 40.88 | 24.36 | 39.46 | 39.01 |

in the pores, or by having many ink-bottle pores (pores with large bodies but narrow necks).

Pore distribution measurements by mercury intrusion can reveal the discontinuous nature of the pore structure. Without silica fume, the pore structure changes with sand/cement ratio, i.e. the coarse pore component [(97→0.875) × $10^3$ nm] increases. Second mercury intrusion shows little difference in the pore distributions (3). When silica fume is added, first mercury intrusion reveals an increase in both the fine pores [(0.0175→0.0029) × $10^3$ nm] and coarse pores; the latter increase further with sand/cement ratio, indicating the interfacial nature of the phenomenon. Second mercury intrusion, however, gives results which are very different from those of first intrusion; these results more closely match the distributions of the specimens without silica fume, except that the amount of coarse pores is greater, and increases with sand/cement ratio. This observation indicates that the mercury intrusion partly breaks the pore structure, entering fairly large pores at high pressures. A false indication of the presence of small pores may thus be inferred. The amount of relatively inaccessible coarse pores increases with sand/cement ratio and with a reduction in $Ca(OH)_2$ content.

Previous work (3,6,13) has related the difference in first and second mercury intrustion to $Ca(OH)_2$ content and pore discontinuity. This work confirms that the phenomenon is also related to the sand interface.

## Conclusions

1. Pores in the (97→0.175) × $10^3$ nm range are formed at the interface of sand aggregate in mortars. These pores increase with sand/cement ratio in mixes both with and without silica fume.

2. Silica fume addition to mortars results in an increase in pores of the (97→0.875) × $10^3$ nm range at the sand-aggregate interface. A portion of these pores is relatively inaccessible.

3. The pore distribution of mortars containing silica fume differs from equivalent mortars without silica fume mainly by having a larger coarse pore component. Differences in permeability are due to a discontinuous pore structure.

4. The large increase in fine pore structure observed on first intrusion with addition of silica fume is really due to large but relatively discontinuous pores.

## Acknowledgements

The author wishes to thank G.W. Chan for his valuable help in performing the experiments. This paper is a contribution of the Division of Building Research, National Research Council of Canada.

## References

1. Huang Cheng-yi and R.F. Feldman, "Influence of Silica Fume on the Microstructural Development in Cement Mortars". Cem. Conc. Res., 15, 285 (1985).
2. R.F. Feldman and Huang Cheng-yi, "Microstructural Properties of Blended Cement Mortars and Their Relation to Durability of Concrete Structures Under Normal Outdoor Exposure", Hanover, 26-29 March 1984 (in press).
3. Huang Cheng-yi and R.F. Feldman, "Dependence of Frost Resistance on the Pore Structure of Mortar Containing Silica Fume". (In press. Amer. Conc. Inst. J.)
4. Huang Cheng-yi and R.F. Feldman, "Hydration Reactions in Portland Cement - Silica Fume Blends". (In press. Cem. Conc. Res.)
5. Bakker, R.F.M., Proceedings, Fifth International Conference on Alkali-Aggregate Reaction in Concrete, Cape Town, South Africa, 1981, National Building Research Institute, Council for Scientific and Industrial Research (1981).
6. R.F. Feldman, Proc. 1st Intern. Conf. on the Use of Fly-Ash, Silica Fume, Slag and Other Mineral By-Products in Concrete, ACI SP 79, Vol. I, 415 (1983).
7. M. Regourd and B. Mortureux, Proc. 4th Intern. Conf. on Cement Microscopy, Las Vegas, USA, 249 (1982).
8. P.K. Mehta and O.E. Gjorv, Cem. Conc. Res. 12, 587 (1982).
9. B.D. Barnes, S. Diamond and W.L. Dolch, J. Amer. Ceram. Soc. 62, (1-2), 21 (1979).
10. A. Carles-Giberques, J. Grandet and J.P. Olliver, Proc. Intern. Conf. on Bond in Concrete. Paisley College of Technology, Scotland, London (Appl. Sci.) 24 (1982).
11. R. Berger, D.S. Cahn and J.O. McGregor, J. Amer. Ceram. Soc. 53, (1), 57 (1970).
12. R.Sh. Mikhail and A.M. Youssef, Cem. Conc. Res. 4, (6), 869 (1974).
13. R.F. Feldman, J. Amer. Ceram. Soc. 67, 30 (1984).